Astron. Astrophys. 356, 146–156 (2000)

ASTRONOMY AND ASTROPHYSICS

A spectroscopic study of the magnetic CP-star HR 1094⋆

K. Nielsen and G.M. Wahlgren

Atomic Spectroscopy Group, Department of Physics, University of Lund, Box 118, 221 00 Lund, Sweden
(krister.nielsen@fysik.lu.se; glenn.wahlgren@fysik.lu.se)

Received 28 October 1999 / Accepted 8 February 2000

Abstract. The chemically peculiar star HR 1094 has been investigated with respect to its chemical composition and the magnetic influence on its stellar spectrum. By using spectral lines slightly affected by the field $v \sin i$ was determined to be ≤ 17 km s^{-1}. The iron-group elements as well as chlorine and the heavy elements platinum, gold and mercury show an overabundance compared to the sun. The analysis also revealed the rare earth elements to be present from lines of their second and third spectrum.

Key words: line: profiles – stars: abundances – stars: chemically peculiar – stars: individual: HR 1094 – stars: magnetic fields

1. Introduction

HR 1094 (=HD 22316) has been classified as a B9p star (Hoffleit & Jaschek 1982) with strong spectral lines of chromium (Cowley et al. 1969) and silicon (Palmer et al. 1968). Its spectrum also displays more pronounced characteristics such as strong Co, Cl and Hg lines. In an earlier analysis (Sadakane 1992) HR 1094 was investigated with respect to its chemical composition, with results revealing the star to have an abnormally high abundance of Co and Cl, while other elements such as Si, Mg and Ca were found to be underabundant relative to the sun. This analysis was limited to a small number of elements, mostly from the iron group.

HR 1094 was proposed to be an Ap star by Hill & Blake (1995), based on polarisation measurements in the H$_\beta$ line wings, however, the magnetic field is not large enough to produce resolved Zeeman components. Hill & Blake determined the observed longitudinal magnetic field to be time variable with an amplitude of 2.0 kG and a period of approximately 3 days. The angle between the rotational and the magnetic axes, β, was estimated to be 76°. These results were based on a stellar atmosphere model from Sadakane, including a value for the rotational velocity ($v \sin i$). Since the signal-to-noise ratio (S/N) of Sadakane's photographic spectrum was rather low, Hill & Blake stressed the importance of obtaining spectra of higher quality in order to determine $v \sin i$ more accurately.

The influence of a magnetic field has been typically neglected in stellar spectrum analyses for chemical abundances. In the absence of observed resolved Zeeman line splitting, slightly broadened lines analyzed under the assumption of negligible magnetic field will lead to an overestimate of chemical abundances. One approach to accounting for magnetically increased line equivalent width is by an appropriate increase in the turbulent velocity. This approach may produce the desired increase in absorption but assumes that all atoms/ions are affected in a similar manner by the local magnetic field. More accurate line profile modelling techniques take into consideration the sensitivity of individual spectral lines to a magnetic field through the Landé factors for the transition upper and lower level. Computer codes have been formulated to various degrees that account for polarized radiation transport through model atmospheres for application to magnetic field work in both warm (Landstreet et al. 1989) as well as solar and cooler (e.g. Basri & Marcy 1988; Saar 1988; Valenti et al. 1995) stars. Our synthetic spectrum analysis addresses the individual Zeeman line broadening in a simpler manner, with each component treated as an individual spectral line undergoing unpolarized radiative transport. This approach is similar to that one employs for individual hyperfine or isotopic components of a line and allows us to explore the gross nature of the magnetic field and its effect upon spectral line profiles.

Our main reasons for conducting further investigation of HR 1094 were to confirm the curious abundance enhancement for Co and Cl, and to extend the abundance analysis to additional elements, for example the rare-earth elements (REE) and the heavy elements of the platinum group to better characterize a potentially different elemental abundance distribution. This initial line of inquiry lead to other paths as we realised that the magnetic field had a greater influence upon the line widths than we had anticipated.

In this paper we investigate elemental abundances for the magnetic, chemically peculiar (CP) star HR 1094 and incorporate an approximated treatment of the line structure for selected lines in order to explore the nature of the magnetic field. Since our ground-based spectra are of higher S/N and spectral resolu-

Send offprint requests to: K. Nielsen

⋆ Based on observations obtained with the Nordic Optical Telescope, operated on the island of La Palma jointly by Denmark, Finland, Iceland, Norway, and Sweden, in the Spanish Observatorio del Roque de los Muchachos of the Instituto de Astrofísica de Canarias.

tion than that used by Sadakane, it was also possible to determine a more accurate value of $v \sin i$.

The southern magnetic star HR 5049 (=HD 116458, spectral type A0p (Hoffleit & Jaschek 1982)), has similar characteristics as HR 1094 and is therefore presented for comparison. Both stars show an enhancement of cobalt and have a measurable magnetic field. HR 5049 has sharper spectral features and a stronger field than observed for HR 1094, consequently the effects of some characteristics are more distinct in the spectrum of HR 5049.

The A1V (Hoffleit & Jaschek 1982) star HR 3383 (=HD 72660) is also used for comparison in the rotation velocity analysis since it is a sharp-lined star with a more solar-like chemical composition.

2. Observations

Our optical data were obtained with the Nordic Optical Telescope (NOT) at La Palma, Canary Islands, using the SOviet FINnish high-resolution echelle spectrograph (SOFIN) at resolving powers $R = \frac{\lambda}{\Delta\lambda}$= 170 000 (camera 1) and 85 000 (camera 2). HR 1094 was observed on two different occasions, in November 1995 and in April 1998. In total, 12 orders of camera 1 spectra (JD 2450418.478, ϕ = 0.073) with S/N of 50, and 44 orders of camera 2 spectra (JD 2450417.414, 2450911.331, 2450911.350 and 2450919.344 at respective phases ϕ = 0.712, 0.677, 0.683 and 0.369) with S/N between 95 and 190 were obtained during the two observation runs. All observations required an exposure time of approximately 20 minutes. The spectral coverage between 3800 and 6500 Å was not complete. The instrumental profile is treated as a gaussian, which except for a discrepancy in the line wings at the low level of 0.1% is a good approximation. The errors in the ephemeris of Hill & Blake restrict us from predicting the phase of our observation accurately. However, we have chosen to use their relation to denote a phase for the abundance analysis.

The purpose of the initial observation was to investigate the chemical composition of HR 1094, however, preliminary results indicated an influence of the magnetic field upon lines that exhibit a simple Zeeman pattern. Obtaining additional spectra allowed us to observe magnetically unaffected lines to determine the rotational velocity more accurately, as well as strong lines of Cl II which were not originally recorded.

In April 1998 we gathered the additional spectra, but the conditions for observing HR 1094 were not optimal. The object was only observable at the beginning of the night due to its low altitude. Observations below an altitude of approximately 30° increase the air mass quickly. The flexure of the spectrograph may become pronounced for observations near the horizon. The total observation time was less than two hours per night, during which time 30 orders of spectra were obtained, all of them with camera 2. The observational material covered three different grating settings, one defined to analyse the above mentioned Cl II lines, another included the Mg II line complex at 4481 Å and Fe II lines little affected by the magnetic field. The third and last region was defined to observe the Fe II lines near 6150 Å, often used to investigate the influence of a magnetic field in a stellar spectrum. The latter two spectral regions were located off the blaze, and since the star was dropping toward the horizon, the exposure was divided into three segments to check for possible effects of flexure. The different exposures were co-added and compared with the individual observation sets. The line profiles for the individual exposures were identical and the concern regarding flexure could be neglected.

Many elements of astrophysical interest do not have strong transitions in the optical wavelength region, and ultraviolet spectra can be included to complement the analysis. We have thus used high-dispersion spectra of HR 1094 obtained with the International Ultraviolet Explorer (IUE) satellite with an approximate resolving power of 12 000 in addition to our ground based material. The IUE material is a co-added spectrum of five images, reduced using NEWSIPS software, from IUE observing program MMPSA of S. Adelman (The Citadel) and G.M. Wahlgren.

HR 5049 is not visible from the NOT. The spectrum of this star was obtained with the ESO New Technology Telescope (NTT) at La Silla, Chile, and provided to us by G. Mathys (ESO). The observational material consists of a continuous spectrum between 4100 and 6700 Å at a resolving power of 60000.

During the NOT observation run in April 1998, spectra of the star HR 3383 were also obtained. The material used in this paper were obtained with camera 2 at a S/N of 95.

3. Atmospheric models

The determination of stellar parameters has been accomplished through the application of the uvbybeta photometric calibration of Moon & Dworetsky (1985) as improved by Napiwotzki et al. (1993). Hoffleit & Jaschek identified HR 1094 to be of B9V spectral classification but Hill & Blake measured a magnetic field and classified it as an Ap star. A recent photometric study (Adelman 1999) implies the photometric $uvby$ colour variations to be approximately $\pm$0.01 magnitude over the rotational period. This colour amplitude translates into a temperature variation of $\pm$ 300 K, using the calibration by Napiwotzki et al., which is typically within the error margins of the temperature determination for B-type stars.

If both HR 1094 and HR 5049 have effective temperatures exceeding 9500 K we can assume β to be a suitable gravity indicator while the c_1 or $(u - b)$ index measures effective temperature. The Johnson (U - B) and (B - V) indices for HR 1094 are taken from Haggkvist & Oja (1969) while corresponding indices for HR 5049 and HR 3383 are from Johnson et al. (1966). All Strömgren indices were taken from Hauck & Mermilliod (1980). We used expressions developed by Napiwotzki et al., based on a reference frame of Ap stars, to determine an effective temperature for HR 1094 of 12 000 K. Moon & Dworetsky presented a calibration grid of the surface gravity using the β index. From this grid HR 1094 is assign a $\log g$ of 4.2 $\pm$ 0.2, where the error margin is an estimated read-out uncertainty.

Similar calculations have been performed for HR 5049 and HR 3383 yielding $T_{\rm eff}$= 10 500 K and a $\log g$= 4.0 for

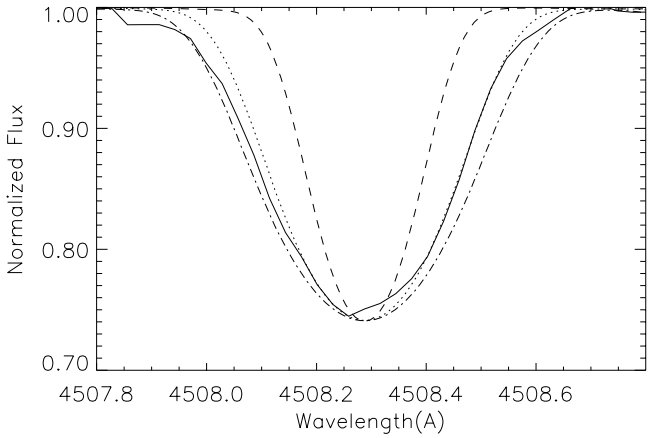

Fig. 1. Determination of the rotational velocity for HR 1094 with the Fe II λ4508 line. Solid curve: observed profile. The best fit synthetic profile is computed with $v \sin i$=17 km s^{-1} (dotted) and compared with profiles computed with $v \sin i$ =10 km s^{-1} (Sadakane, dashed) and 20 km s^{-1} obtained using the Mg II λ4481 line (dash-dot).

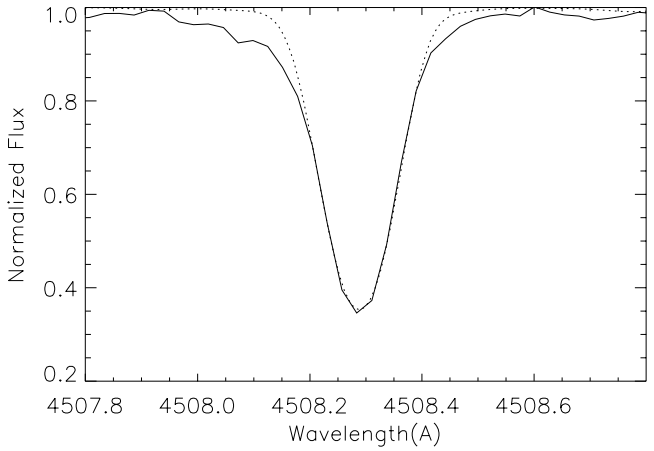

Fig. 2. Determination of the rotational velocity for HR 5049 using the Fe II λ4508 line. Solid curve: observed profile. Dotted curve: synthetic spectrum generated with $v \sin i$=4 km s^{-1}.

HR 5049 and $T_{\rm eff}$= 9 750, log g= 4.0 for HR 3383. For each star an interpolated model was chosen from the ATLAS9 grid of Kurucz (1993) under the assumption of no turbulent velocity.

4. Determination of the rotational velocity

In order to perform an accurate abundance analysis via synthetic spectrum fitting, it is of great importance to use a well-determined rotational velocity ($v \sin i$). This work is based on a rotation alvelocity determined by fitting individual spectral lines with those calculated by the synthetic spectrum program SYNTHE (Kurucz 1993). Ideally, the spectral lines chosen for such an analysis should not be broadened by hyperfine structure (hfs), isotopic shift (IS), Zeeman effect and line blending unless these effects can be modelled.

The effect of hfs originates from the interaction between nuclear spin and the angular momentum of the electrons. It is absent for those atoms with an even mass number, as these isotopes do not have a net nuclear spin. If the star is assumed to have the same isotopic mixture as our solar system, then iron is highly concentrated to one isotope (92% ^{56}Fe). Therefore, iron lines do not show significant hyperfine structure or isotopic shift and are particularly useful when investigating rotational velocities. However, in the presence of a magnetic field the spectral lines may be broadened by the Zeeman effect. How much the spectral lines are affected by the magnetic field depends on the magnitude of the field, the transition wavelength and the Landé factors for the corresponding energy states. If we have transitions where both the upper and lower energy level have Landé factors equal to zero, the spectral line will be unaffected by the magnetic field. Ideally these lines should be used when investigating the rotational velocity for magnetic stars. We prefer to use iron lines to avoid IS and hfs and are then constrained to transitions between ^{4}D$_{1/2}$ and ^{6}G$_{3/2}$ states. These energy levels have Landé factors equal to zero, which is confirmed by experimental measurements (g $<$ 0.05) (Moore 1971). Unfortunately, there are few unblended transitions corresponding to these levels, and we have not been able to use any magnetically unaffected spectral lines since they are weak and blended. There are a few useful spectral lines which correspond to energy levels with relatively small Landé factors (g $\leq$ 0.5), and since they are located in the blue wavelength region the Zeeman effect is reduced relative to longer wavelengths. The Fe II λ4508 and λ4491 lines are both unblended for stars with solar-like elemental abundance distributions and little affected by the magnetic field.

The rotational velocity for HR 1094 was determined to have an upper limit value of 17 km s^{-1}, using the Fe II line at 4508 Å. As shown in Figs. 1 and 2 the iron line appears to be only slightly blended in the blue wing, and therefore a good choice for this purpose. The error margin is estimated to be less than 1 km s^{-1}, based on the visual appearance of the synthetic spectrum fits to that part of the observed profile not apparently affected by the noted blend. HR 1094 is observed to have a reasonably high rotational velocity and a magnetic field with a small magnitude, consequently the rotation is the dominating broadening mechanism for its spectrum. For stars with a more dominating magnetic field and a lower rotational velocity, for example HR 5049, special care should be taken when choosing lines for investigating the rotational velocity, since the field is capable of changing the line profile dramatically. The Zeeman components have been included in our synthetic spectrum analysis, regardless of whether the spectral lines Fe II λ4491 and λ4508 are significantly broadened by the magnetic field.

HR 5049 presents a sharp-lined spectrum with a mean magnetic field of 4676 G (Mathys et al. 1997), and as shown in Fig. 2 the Fe II λ4508 line is also useful for the analysis of this object. The rotational velocity for HR 5049 was determined to be 4 km s^{-1}. Dworetsky et al. (1980) suggested $v \sin i$ to be less than 6 km s^{-1} which is in agreement with our result. The magnetic field is determined to influence the value of the rotational velocity by less than 0.5 km s^{-1}. The Fe II λ4491 line has a Co II line in its short wavelength wing, which jeopardises the inves-

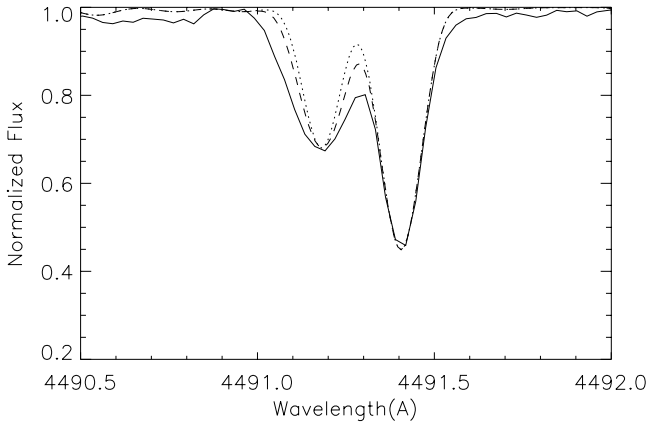

Fig. 3. Determination of the rotational velocity with the Fe II λ4491 line. HR 5049 is an slow rotator, hence the Fe II and the Co II lines are resolved and the peculiar line profile of the Co II line is visible. Solid profile: observed curve. Both synthetic spectra are generated with $v \sin i$=4 km s^{-1}. The dotted line is without and the dashed with the Zeeman structure.

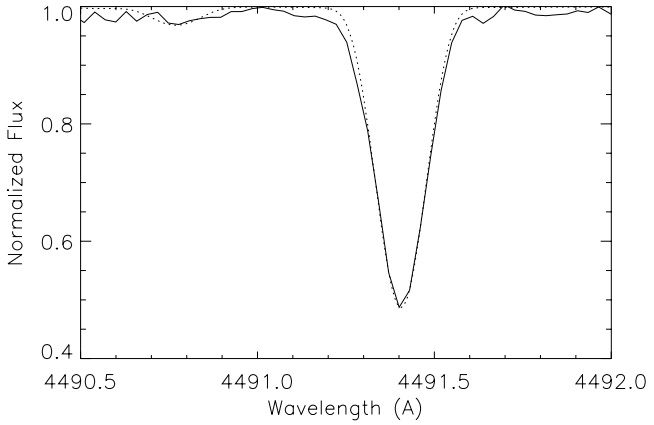

Fig. 4. For HR 3383 the cobalt abundance is solar and the Fe II λ4491 line is a good choice for the investigation of $v \sin i$. Solid curve: observed profile. Dotted curve: synthetic profile computed with $v \sin i$=6.5 km s^{-1}.

tigation of $v \sin i$. For slow rotational velocity stars ($v \sin i \leq$ 10) observed at high spectral resolution, the Co II line and the Fe II line are resolved. The influence of the magnetic field on the line profiles has been investigated by including the Zeeman components in our synthetic spectrum and as shown in Fig. 3 only a small amount of the missing opacity can be explained by the Zeeman effect. We suggest that full knowledge of the hfs pattern for this line in collaboration with the magnetic broadening would fully explain this line profile. For stars with no enhancement of Co II, the Fe II line at 4491 Å is suitable for accurately determining the rotational velocity, as exemplified by the spectrum of HR 3383 in Fig. 4.

In the analysis of HR 1094 by Sadakane the rotational velocity, $v \sin i$, was taken to be less than 10 km s^{-1}. This value was obtained by using the observed FWHM for the Mg II λ4481 line in a reference frame compiled by Sletteback et al. (1975). Outside of using synthetic spectra a determination of $v \sin i$ is

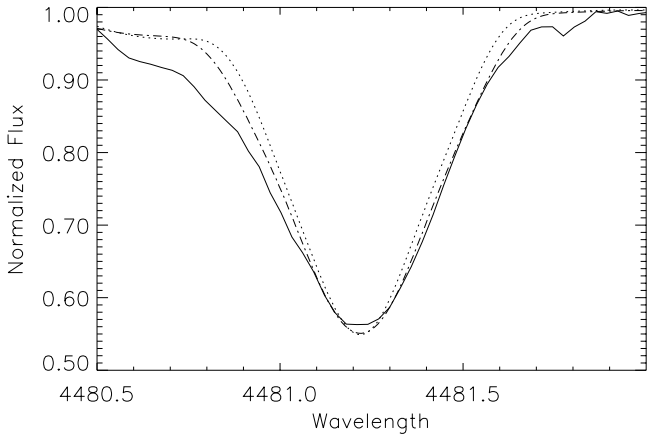

Fig. 5. Analysis of $v \sin i$ for HR 1094 using the Mg II λ4481 line. The solid curve representing the observed profile is compared with synthetic spectra generated with $v \sin i$=17km s^{-1} (dotted) and 20 km s^{-1} (dash-dot).

often dependent on strong unblended lines such as Mg II λ4481 that are calibrated by a reference frame of standard stars. The risk in using such frames is the necessity to be sure that only stars similar to the investigated object are used for the reference frame.

For completeness, we have also analyzed the Mg II λ4481 feature in the spectrum of HR 1094 (Fig. 5). The result obtained by using this line is in disagreement with that obtained from unblended Fe II lines. From the Fe II lines used $v \sin i$ was determined to have an upper limit of 17 km s^{-1}. The corresponding value from the Mg II line is 20 km s^{-1}. The 3 km s^{-1} difference is too large to be within the error margins of the determination. The modelled Mg II feature is actually three lines from the same multiple (3d ^{2}D – 4f ^{2}F). For HR 5049 and HR 3383 the analysis using this feature yields a smaller value of $v \sin i$ than obtained from unblended Fe II lines. It is difficult to simultaneously fit the Mg II feature in both depth and width, which may be a consequence of the failure of the local thermodynamic equilibrium assumption of the calculations. Other explanations might be isotopic shift, hyperfine structure or Zeeman effect. Magnesium has three stabile isotopes and their relative abundances are, ^{24}Mg : ^{25}Mg : ^{26}Mg = 79 : 10 : 11, where only one of the isotopes possesses hfs. The strength of the Landé factors for the upper (g_J=2.5, 3.5) and lower (g_J=1.5, 2.5) (Moore 1971) levels for the transitions implies a noticeable Zeeman structure, but the wavelength of the spectral feature indicates this effect to be negligible. Since it is difficult to account for all above mentioned effects, the use of the Mg II λ4481 Å is not recommended for the most accurate determination of $v \sin i$.

5. Magnetic line structure

Isotope shift, hyperfine structure and the Zeeman effect complicate the depth and breath of the line profiles, and to use spectral lines influenced by any of these effects without accounting for them in the model may add a systematic error to the result. The IS and the hfs are dependent on atomic characteristics and

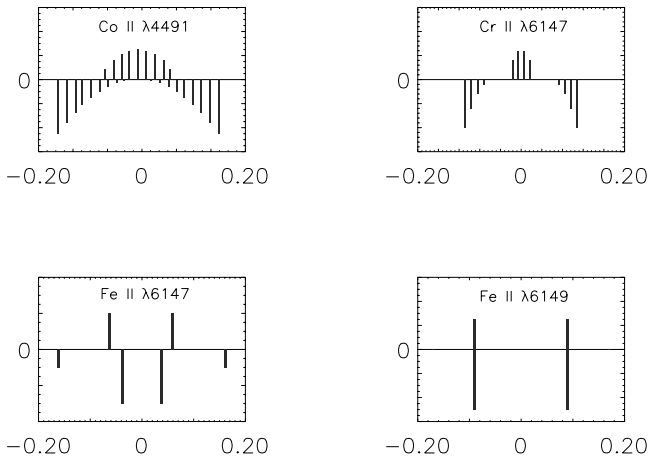

Fig. 6. Zeeman pattern for different spectral lines discussed in this paper. The patterns are computed for B=4676 G, which is the average magnetic field for HR 5049. The shift of the individual components are in Å with the π components above and the $\sigma_\pm$ components below the x-axis.

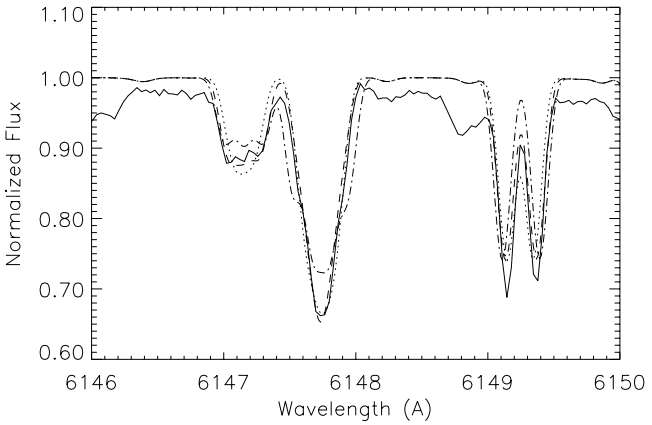

Fig. 7. Investigation of the influence of the magnetic field in HR 5049. Solid curve: observed spectrum. Synthetic spectra are generated for B=4000 (dotted), 4676 (dashed) and 6000 (dash-dot).

are therefore possible to account for in the model by including the appropriate atomic data. In the presence of a magnetic field most spectral lines will be broadened by the interaction between the electrons and the external magnetic field, referred to as Zeeman effect. The observed effect is dependent upon the structure, orientation and magnitude of the magnetic field on the stellar surface as viewed at the epoch of the observation.

If we can restrict the analysis to elements not significantly affected by IS and hfs, then the Zeeman effect can be analyzed independently. The Zeeman splitting can be resolved if unblended lines with simple Zeeman pattern are observed in slowly rotating stars with an appropriately high spectral resolving power. The Zeeman components have different polarisation states. Viewed along the direction of the magnetic field, the π components vanish while the circularly polarized $\sigma_\pm$ components and their relative wavelength shift are measurable. When viewed at some random angle to the field the line profile will have contributions from all polarisation states. If the Zeeman components are resolved it is possible to measure the separation of the $\sigma_\pm$ components and calculate the strength of the magnetic field.

Hill & Blake analyzed the magnetic field for HR 1094 by investigation of polarized radiation in the H_β line wings and determined the phase dependent effective longitudinal field (Landstreet 1982) strength, B_e, for HR 1094 to be:

$$B_\mathrm{e} = B_0 + B_1 \sin 2\pi(\phi - \phi_0) \quad (1)$$

where B_0 and B_1 are constants with the values (-834 ± 218) and (1396 ± 415) G, respectively, and ϕ the phase where magnetic maximum occurs at phase ϕ_0=0.75. This expression corresponds to a period of 2.9761 ± 0.0014 d. We have calculated B_e at the second observation time (JD 2450919.344) for HR 1094 to be 1800 G using equation Eq. 1. The ephemeris provided by Hill & Blake can only be used as an indication of the field strength due to its uncertainty. The field strength for HR 5049 is 4676 G (Mathys et al. 1997) with little time variation.

Magnetic line broadening is linearly proportional to the magnetic field strength, the Landé factor, g_J, and quadratically with the wavelength. Consequently, there is a better chance of observing Zeeman splitting in the red spectral region than at bluer wavelengths. The Fe II lines at 6147 and 6149 Å are often used to investigate the influence of the magnetic field in warm stars, where the resolved component separation for Fe II λ6149 provides a measurement of the mean magnetic field modulus (Mathys 1990). These lines occur in the same multiplet, are formed at the same atmospheric depth and have nearly identical oscillator strengths. Therefore, their line depths are similar in the absence of a magnetic field. However, line blending and spectral resolution may play a role in their observed appearance. Both spectral lines have the same upper level, $z\,^4P_{1/2}$, which is divided into two sublevels when affected by a magnetic field. The transitions have lower levels with unequal g_J, which results in different Zeeman patterns. The Fe II λ6149 line has a simple Zeeman pattern with only two resolved features, each composed of a π and a σ component while Fe II λ6147 shows a more complicated structure. For an appropriately high abundance of chromium the line Cr II λ6147 is observable just bluewards of Fe II λ6147. This feature also shows a complicated Zeeman pattern. Chromium has four stable isotopes, one of them with hfs. The intensity ratio of the isotopic components is approximately, ^{50}Cr : ^{52}Cr : ^{53}Cr : ^{54}Cr = 84 : 10 : 4 : 2, and the wavelength shift between the outermost components is estimated to be less than 20 mÅ. Both the IS and the hfs are less significant for chromium and the profile shown in Fig. 7 is exclusively the result of the Zeeman effect.

We have investigated the Zeeman structure for four lines with respect to wavelength and intensity for the individual components, and the complete pattern has been included in our line list data for specific magnetic field strengths. As we not are certain of the magnetic field orientation relative to the line of sight, we chose the field to be oriented in such a manner that the π and $\sigma_\pm$ components are equally observable. In this case the compo-

Table 1. Spectral lines investigated in this paper with respect to the Zeeman effect.

		Lower level			Upper level				
Ion	λ_0	Conf.	E (cm^{-1})	g_J [a]	Conf.	E (cm^{-1})	g_J [a]	log gf	REF.
Co II	4491.184	c^3F_4	41047.060	1.251	c^3H_5	63306.660	1.037	−2.877	K88
Cr II	6147.154	$c^4D_{3/2}$	38362.430	1.200	$z^4D_{5/2}$	54625.620	1.376	−2.843	K88
Fe II[b]	4491.398	$b^4F_{3/2}$	23031.300	0.398	$z^4F_{3/2}$	45289.801	0.455	−2.700	FMW
	4508.282	$b^4F_{3/2}$	23031.300	0.398	$z^4D_{1/2}$	45206.450	−0.021	−2.210	FMW
	4923.922	$a^6S_{5/2}$	23317.635	1.996	$z^6P_{3/2}$	43620.981	2.398	−1.320	FMW
	6147.714	$b^4D_{3/2}$	31364.440	1.200	$z^4P_{1/2}$	47626.105	2.700	−2.721	K88
	6149.238	$b^4D_{1/2}$	31368.455	0.000	$z^4P_{1/2}$	47626.105	2.700	−2.724	K88

[a] Moore, C.E.,1971

[b] Wavelengths and energy levels for Fe II lines from Johansson, S., private communication

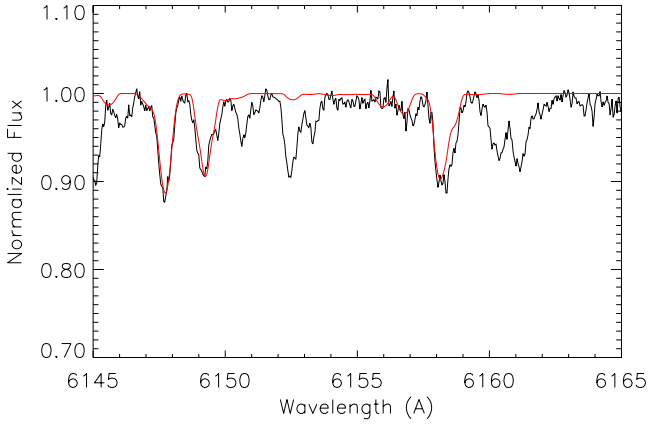

Fig. 8. Investigation of the magnetic field for HR 1094, using the Fe II lines at 6150 Å. Solid curve: observed spectrum. Synthetic spectra generated for 6000 G (dashed).

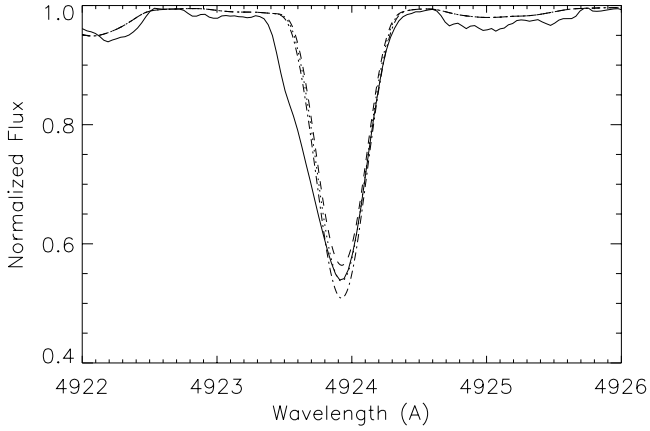

Fig. 9. Determination of the magnetic field strength for HR 1094. Solid curve: observed spectrum. Synthetic spectra generated for 2000 G (dashed), 2500 G (dotted) and 3000 G (dash-dot).

nents will be as shown in Fig. 6, where the Zeeman pattern is presented for four spectral features with notably different distributions of the Zeeman components. If the orientation of the field is altered the spectral lines will be affected individually, the Co II and the Cr II lines have their π components centred and if they are removed a high point at the centre will show in the line profile. Since the spectral lines are affected differently we can obtain information about the magnitude and the orientation of the magnetic field by changing the magnetic field strength and the relative intensities of the components included in our model.

The modelling is performed for HR 1094 and compared with a similar analysis of HR 5049. HR 1094 is not an extremely slow rotator and since the magnetic field is weak we did not expect observations of resolved Zeeman components. The spectral features were analyzed in order to see how the line profile changed in a presence of a magnetic field. Unfortunately, Fe II λ6149 appears to be blended with an unidentified feature in its long wavelength wing and may cause problems in an analysis of the line profile and abundance. Hg II λ6150 is not prominent in our spectrum. The Cr II λ6147 and Fe II λ6147 lines are blended due to the large rotation and in order to mimic the depth of the Fe II lines it is necessary to use a Zeeman structure corresponding to a magnetic field of 6000 G (see Fig. 8). Fe II λ4923 is strongly affected by the magnetic field with a similar Zeeman pattern as Co II λ4491. In addition to the blended Fe II λ6149 line this feature is used to determine the magnetic field strength independently of the investigation by Hill & Blake. Fig. 9 shows how the line depth is calculated to grow with increasing magnetic field strength. The iron abundance is constant and obtained from the Fe II λ4508 line. The uncertainty introduced by the blend in the blue wing of the spectral line has been analyzed by adding spectral features to correct for the missing opacity. We have estimated the blend to be accountable for a decrease of the magnetic field by 500 G. The field is determined to be (2000 $\pm$ 200) G, where the error is the accuracy of the synthetic spectrum fitting. Our result seems to be in agreement with that obtained with Eq. 1. It is possible that our values of the field strength are not comparable with the values obtained with Eq. 1, even if we know this expression only gives an approximate value of the field strength. The different techniques do not measure the field in a similar way. Measurements of polarized radiation give an average of the field over the stellar surface and is sensitive to the projected magnetic field. Measurements of line profiles made by including Zeeman components are sensitive to the magnetic field modulus. The result for the field strength obtained with the

Fe II lines at 6150 Å can not be ignored since the analysis of the magnetic field for those lines are simpler, due to the larger wavelength and their simple Zeeman structure. The unknown nature of the line blend may have a larger effect than believed.

The spectrum of HR 5049 shows Zeeman splitting for Fe II λ6149 and as a result displays a characteristic bottle-shaped profile. Cr II λ6147 is visible in the spectrum of HR 5049 and has also been modelled in our analysis. The magnetic field has been altered to test the sensitivity of the features to changes in the magnetic field. We can confirm the value of the magnetic field for HR 5049 derived by Mathys et al. to an accuracy of $\pm$ 200 G.

6. Abundance analysis for HR 1094

The spectrum for HR 1094 is dominated by spectral lines from the iron-group elements. However, the REE are also prominent, since they have rich line spectra and are relatively abundant. Spectral lines from the iron-group elements, preferably iron lines in the red spectral region, are used to determine the metallicity since these lines are less affected by blending. However, in the presence of a magnetic field the Zeeman broadening is more pronounced in the red spectral region and spectral lines little affected by the field should be used. A metallicity analysis was performed by investigating appropriate iron-group lines, using a solar abundance atmospheric model. This preliminary synthetic spectrum analysis yielded HR 1094 to have a metal abundance five times greater than the sun.

Using an ATLAS9 model based on this enhanced metallicity, the spectral lines for the iron-group elements were analyzed for the entire spectral region with results presented in Table 2 and the corresponding line list in Appendix A. The appropriateness of useful lines is difficult to assess since most lines are blended or affected by either IS, hfs or Zeeman broadening, but their credibility can be estimated by investigating the line profile for possible blends. For determining the iron-abundance, Fe II λ4508 is of special interest since it is less influenced by certain broadening mechanisms and its oscillator strength has been derived experimentally. From Fe II λ4508 the iron abundance, $\log N_{\rm Fe}$, is determined to be 8.05. This is a smaller value compared with results obtained by using other Fe II lines, which emphasises the uncertainties the broadening mechanisms introduced into the abundance analysis. Analysis of transitions from high and low states give different results which might be due to the difficulties in deriving oscillator strengths for highly excited states, but can also be a result of non-LTE effects in the stellar photosphere or a non-uniform temperature distribution. We determined 8.46 to be an average value of $\log N_{\rm Fe}$, which agrees with the value determined by Sadakane within 0.05 dex, yet caution that the interpretation of the iron abundance, like that of all other elements, is not straightforward.

The great overabundance of cobalt is noticeable from the presence of optical region lines. Analysis of the IUE spectrum between 2100 and 2400 Å, which includes the strong Co II λ2286 line, confirms this enhancement. Scandium and nickel do not have strong unblended lines in the investigated spectral region and only an upper limit can be determined.

Table 2. Result of the abundance analysis compared with solar values and the earlier analysis by Sadakane. $\log N_{\rm H}$=12.

Element	Sadakane	Our work	$[N/N_H]_\odot$
He		10.1	−0.9
N		5.5	−2.5
O		8.1	−0.8
Mg	7.25	6.6	−0.9
Si	6.54	6.8	−0.7
Cl	9.34	8.1	+2.6
Ca	5.83	8.0	+1.7
Sc	$\leq$ 3.04	$\leq$ 3.4	$\leq$ +0.4
Ti	6.55	6.69	+1.74
Cr	7.20	7.02	+1.39
Fe	8.45	8.46	+0.83
Co	8.26	7.92	+3.04
Ni	$\leq$ 6.22	$\leq$ 5.8	$\leq$ −0.4
Cu		6.5	+2.3
Zn		$\leq$ 3.5	$\leq$ −1.1
Sr	4.32		
Ba		$\leq$ 3.1	$\leq$ +1.0
Ce		5.2	+3.7
Eu		3.8	+3.3
Gd[a]		4.9	+3.8
Gd[b]		6.2	+5.1
Dy		4.6	+3.5
Er		2.3	+1.4
Pt	6.01	5.4	+3.6
Au		4.0	+3.0
Hg	5.86	4.8	+3.8

[a] ϕ = 0.073
[b] ϕ = 0.677, 0.683

Many chemically peculiar stars are known to be underabundant in helium. He I λ4471 was investigated in order to determine the helium abundance. The analysis used a spectrum provided by S. Adelman (The Citadel) obtained with a resolving power of 35 000, and showed helium to be deficient by 0.9 dex.

Chlorine is a rarely observed element in stellar spectra, and claims of its detection, are therefore always met with caution. Many of the strong spectral lines of Cl II in the optical region are present in our data and a few of them in the same order (Fig. 10). We are able to confirm an overabundance of chlorine but at a reduced level from that proposed by Sadakane.

The heavy elements Pt, Au and Hg are present with abundances similar to the non-magnetic HgMn stars. Mercury has been investigated with respect to its isotope mixture by analyzing the Hg II λ3984 line observed with high resolving power. The isotope structure was analyzed by including the hfs and IS components from Wahlgren et al. (2000) into our synthetic stellar spectrum. The wavelength scale was set relative to Co II λ3983 and Cr II λ3979, and the use of a terrestrial mercury isotope mixture shows a shift in wavelength of approximately 20

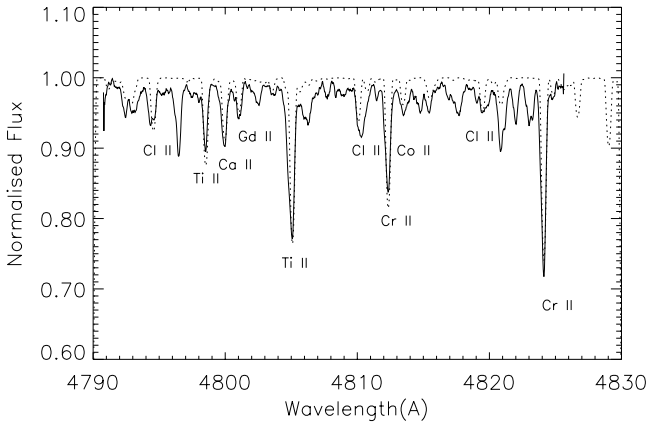

Fig. 10. Due to a large overabundance, spectral lines from chlorine are visible in the spectrum of HR 1094. Solid curve: Observed spectrum. Synthetic spectrum generated with chlorine abundance enhanced by 2.6 dex relative to the sun.

mÅ. The wavelength calibration is set with an accuracy of ± 10 mÅ, based on errors in the determination of the energy levels for chromium (Sugar & Corliss 1985). This shift may be explainable by magnetic broadening in addition to a wavelength shift but the magnetic influence is not expected to be great at this wavelength and another explanation is preferable. One possible explanation of the wavelength shift is if the isotope mixture consists only of the isotopes ^{200}Hg, ^{201}Hg and ^{202}Hg. The Hg II λ1942 line was investigated in the IUE spectrum, using the isotopic structure presented by Leckrone et al. (1991) for terrestrial mixture, to confirm the presence and the abundance of mercury. The isotopic mixture can not be confirmed due to the low resolving power of the IUE data. A similar isotope investigation for Pt II λ4046 was made with isotopic structure from Wahlgren et al. (2000), but such information was not possible to extract since the weak Pt II λ4046 line is blended with spectral lines from REE.

N I λ1742 and λ1745 indicate a reduced abundance of nitrogen of three orders of magnitude compared to the solar value. Oxygen was mainly analyzed from the O I triplet at 6156 Å and shows an underabundance of approximately 0.8 dex compared to the sun. The strong C I lines in the UV wavelength area were severely blended and the C II lines are too weak to use for an accurate abundance analysis. All carbon lines implied carbon to be underabundant by at least one order of magnitude.

Analysis of the spectrum for HR 1094 showed that the REE were represented by lines from their second spectra. Since HR 1094 is reasonably hot and the REE have low ionisation potentials, it seems likely that third and possibly fourth spectrum lines could also be present. If the presence of different ions is dependent only on the effective temperature and the electron density, then the third spectrum should be the most prominent with spectral lines corresponding to transitions between low excited states. The fourth spectrum might be observable but with present atomic data no lines were identified in the optical region. Most of the strong spectral lines from the REE in the optical region are severely blended. Observations made in the near-UV would increase the accuracy of the abundance analysis, since the REE (e.g. Ce III, Pr III and Gd III) have many strong spectral lines between 3100 and 3600 Å. But analyses made for some of the REE, in particular gadolinium, show strong unblended spectral lines from both the second and the third spectrum. We have for an abundance analysis usable Gd II lines from both of our NOT observations, which show the abundance of gadolinium to differ by approximately one order of magnitude. The observations were made at different rotational phases and the difference in abundance may be due to an inhomogeneous gadolinium abundance over the stellar surface. A contributing factor to the observed gadolinium abundance variation with phase may come from potential systematic errors in the oscillator strength data of Meggers et al. (1975). Since phases, ϕ= 0.073 and ϕ= 0.677, 0.683 utilize different wavelength intervals.

7. Conclusions

The magnetic chemically peculiar star HR 1094 has been investigated using optical and ultraviolet spectral data from the viewpoints of its elemental abundances and the stellar properties rotation velocity and magnetic field strength. A common theme has been that the choice of spectral lines is an important factor in both the interpretation and systematic reduction of errors. By choosing spectral lines that are little affected by Zeeman broadening, we have determined the rotational velocity of HR 1094 to have an upper limit of $v \sin i \leq 17$ km s^{-1}. It has been shown that an earlier determination (Sadakane, $v \sin i$ = 10 km s^{-1}) does not reproduce observed line widths. This increase in rotational velocity implies that the value of the inclination, i, is underestimated by Hill & Blake.

Abundance enhancements of the elements chlorine and cobalt are confirmed to be at levels unusually high, apparently even for chemically peculiar stars. However, only a relatively small number of magnetic B-type stars have been scrutinized for their abundance distributions relative to their Ap type counterparts and it therefore remains unclear as to the prevalence of the enhancements for lines of these elements. One can speculate as to whether a strong cobalt line enhancement is related to the presence of a magnetic field. The two cobalt-strong B-type stars (HR 1094, HR 5049) are known to be magnetic, and the cooler roAp stars also show strong cobalt line enhancements (Gelbmann 1998). It may therefore be of some merit to investigate a threshold Co II line strength that identifies the presence of a measurable magnetic field.

The inclusion of additional elements in the abundance analysis, particularly the heavier elements, presents an abundance distribution that is familiar to many chemically peculiar stars: deficiencies for light elements such as helium and nitrogen, enhancements of the iron-group elements, with an still increased abundances for heavier elements. The influence of the magnetic field upon the abundances has not been accounted for in this analysis and may thus lead to overestimates for spectral lines where the Zeeman broadening is particularly large. Likewise, the mixture of spectral data from different phases may also contribute to deviations of the general abundance pattern from that

at any specific phase. However, we note that only for the element gadolinium do we notice a distinct difference in the abundance at different rotational (magnetic) phases. Yet even this difference may be influenced by the goodness of the oscillator strengths of the lines employed in the analysis, as generally weaker lines were observed during 1998 than in 1995.

We have investigated the magnetic field strength of HR 1094 by including the Zeeman components of several spectral lines in a spectrum synthesis analysis. The relative depths of the Fe II λ6147 and λ6149 lines are well fit by a field strength of 6 kG, in contrast to the value of 2 kG at the same phase based upon polarization measurements addressing the field longitudinal component. Our fitting of spectral lines is somewhat analogous to measurement of the mean magnetic field modulus (Mathys 1990) for stars presenting resolved magnetic components. In the case of HR 1094 the rotational velocity is high enough to blend the Zeeman pattern for Fe II λ6149 and we extract the field strength from the relative depths of the two Fe II lines. Confidence in this approach is garnered from the good fit to these lines for the star HR 5049 when using the mean magnetic field value of Mathys et al. Mathys et al. (1997). Providing that the instrumental resolution and stellar rotational velocity are known, the synthetic spectrum fitting procedure can also provide plausible results for marginally resolved Zeeman components by inherently accounting for shifts of the observed component wavelengths that result from the overlapping profiles of the individual components.

Acknowledgements. We acknowledge G. Mathys (ESO) and S. Adelman for supplying data used in this analysis. We are grateful to I. Ilyin for reducing the NOT data and helping us during the observations on La Palma, as well as S. Shore and referee F. Leone for useful comments on the text.

Appendix A: Line list – HR 1094

Ion	λ (Å)	log gf	REF.	log N_Z [a]
He I	4471.473	−0.278	WSG	10.10
N I	1742.731	−0.720	DBG	5.50
	1745.249	−1.119	DBG	5.45
O I	4368.193	−2.720	WSG	7.90
	4368.242	−2.030	WSG	7.90
	4368.258	−2.250	WSG	7.90
	6155.961	−1.401	WSG	8.00
	6155.971	−1.051	WSG	8.00
	6155.989	−1.161	WSG	8.00
	6156.737	−1.521	WSG	8.10
	6156.755	−0.931	WSG	8.10
	6156.788	−0.731	WSG	8.10
	6158.149	−1.891	WSG	8.25
	6158.172	−1.031	WSG	8.25
	6158.187	−0.441	WSG	8.25
Mg II	4481.126	0.740	KP	6.60
	4481.150	−0.560	KP	6.60
	4481.325	0.590	KP	6.60
Si II	4128.054	0.316	BBCB	6.75
Si II	5055.984	0.593	SG	6.70
	5941.024	0.291	SG	6.85
	5978.930	0.004	SG	6.95
Cl II	4794.556	0.455	WSM	7.90
	4811.609	−0.080	WSM	8.10
	4819.480	0.064	WSM	8.10
	4896.783	0.460	WSM	7.88
	5423.257	0.260	WSM	8.35
Ca II	4799.973	−0.469	K88	7.95
Ti II	4350.834	−1.400	MFW	7.50
	4367.659	−1.270	MFW	6.73
	4443.794	−0.700	MFW	6.10
	4444.558	−2.030	MFW	6.65
	4450.482	−1.450	MFW	6.60
	4533.969	−0.770	MFW	6.30
	4629.279	−2.240	MFW	6.30
	4708.665	−2.210	MFW	6.85
	4805.085	−1.100	MFW	6.95
	4911.193	−0.340	MFW	6.95
	5262.137	−2.106	K88	6.55
	5268.615	−1.620	MFW	6.75
	5381.015	−2.080	MFW	6.70
Cr II	3979.505	−0.731	K88	6.70
	4054.076	−2.590	MFW	6.60
	4275.567	−1.709	K88	7.03
	4284.188	−1.864	K88	7.00
	4618.803	−1.110	MFW	7.45
	4634.070	−1.240	MFW	6.85
	4812.337	−1.800	MFW	6.90
	4824.127	−1.220	K88	7.15
	4901.623	−0.826	K88	7.15
	4912.462	−0.948	K88	7.05
	5237.329	−1.160	MFW	6.75
	5502.067	−1.990	MFW	7.22
	5508.606	−2.110	MFW	7.10
	5510.702	−2.452	K88	7.28
Fe II	4122.668	−3.380	FMW	8.30
	4258.154	−3.400	FMW	8.35
	4273.326	−3.258	K88	8.33
	4278.159	−3.816	K88	8.43
	4351.769	−2.100	K88	8.30
	4357.584	−2.113	K88	8.25
	4361.247	−2.114	K88	8.28
	4416.830	−2.600	FMW	8.32
	4451.551	−1.844	K88	8.22
	4508.288 [b]	−2.210	FMW	8.05
	4520.224	−2.600	FMW	8.35
	4541.524	−3.050	FMW	8.35
	4635.316	−1.650	FMW	8.30
	4731.453	−3.360	FMW	8.20
	4908.151	−0.304	K88	8.70
	4913.292	0.012	K88	8.80
	4923.927 [b]	−1.320	FMW	7.85
	5004.195	0.497	K88	8.80
	5018.440	−1.220	FMW	8.70
	5035.708	0.606	K88	8.77
	5247.952	−0.523	K88	8.62
	5251.233	0.507	K88	8.73
	5253.641	−0.091	K88	8.52
	5254.929	−3.227	K88	8.54

Ion	λ (Å)	loggf	REF.	log N_Z [a]
Fe II	5257.122	0.032	K88	8.74
	5258.121	−0.918	K88	8.55
	5260.259	1.069	K88	8.52
	5362.869	−2.739	K88	8.30
	5375.847	−0.291	K88	8.90
	5387.630	0.518	K88	8.45
	5492.079	−0.180	K88	8.55
	5493.833	0.211	K88	8.63
	5506.195	0.950	FMW	8.68
	5529.053	−0.250	K88	8.60
	5643.880	−1.458	K88	8.48
	5645.392	0.085	K88	8.63
	5648.904	−0.242	K88	8.65
	5651.575	−0.580	K88	8.70
	5780.128	0.325	K88	8.55
	5783.630	0.206	K88	8.52
	5784.448	0.060	K88	8.62
	5955.508	−2.196	K88	8.10
	5961.705	0.699	K88	8.70
	6084.111	−3.808	K88	7.95
	6103.496	−2.171	K88	8.20
	6456.383	−2.075	K88	8.05
	6841.665	0.405	K88	8.40
	6855.646	0.022	K88	8.50
Co II	3983.023	−2.200	K88	7.70
	4121.270	−2.912	K88	7.75
	4280.644	−2.687	K88	8.25
	4282.184	−1.369	K88	7.85
	4285.268	−3.359	K88	7.75
	4366.110	−2.999	K88	7.95
	4435.322	−2.417	K88	8.05
	4516.663	−2.562	K88	8.15
	4533.212	−1.737	K88	7.90
	4537.918	−3.297	K88	7.75
	4622.100	−2.084	K88	7.85
	4915.423	−3.425	K88	8.10
Cu II	1944.597	−1.116	KP	6.50
Zn II	2062.004	−0.377	AS	$\leq$ 3.50
Ba II	4554.029	0.170	MWY	$\leq$ 3.10
Ce II	3972.068	−0.281	MC	4.80
	3980.890	−0.050	MC	5.30
	3986.646	−1.030	MC	5.20
Ce III	4535.730	−1.913	BO	5.50
Eu II	4129.725	0.204	BKM	3.73
	4205.042	0.117	BKM	3.78
Gd II [c]	4049.885	0.429	MC	4.90
	4053.291	0.233	MC	5.10
	4130.645	0.068	MC	4.95
	4197.061	−0.331	MC	4.70
	4197.691	−0.038	MC	4.65
Gd II [d]	4253.604	−0.489	MC	6.25
	4596.980	−1.229	MC	6.30
	4601.055	−1.008	MC	6.30
	4801.075	−0.873	MC	6.25
Dy II	3978.561	0.360	MC	4.60
Er III	4539.198	−0.315	JFW	2.10
	4540.772	−0.437	JFW	2.50
Pt II	4046.490 [b]	−1.190	DSJ	5.40
Au II	1740.475	0.550	RW	4.00
Hg II	3983.890 [b]	−1.730	MMD	5.20
	1942.313 [b]	−0.140	MIG	4.30

[a] log N_H=12.0
[b] Center of gravity
[c] ϕ = 0.073
[d] ϕ = 0.677, 0.683

AS	Anderson & Sorenson, 1973
BBCB	Berry et al., 1971
BKM	Biemont et al., 1982
BO	Bord et al., 1997
DBG	Dumont et al., 1974
DSJ	Dworetsky et al., 1984
FMW	Fuhr et al., 1988
JFW	Wyart et al., 1997
KP	Kurucz & Peytremann, 1975
K88	Kurucz 1988
MC	Meggers et al., 1975
MFW	Martin et al., 1988
MIG	Migdalek 1976
MMD	Dworetsky, 1980
MWY	Miles et al., 1981
RW	Rosberg & Wyart, 1997
SG	Schulz-Gulde, 1969
WSF	Wiese & Fuhr, 1975
WSG	Wiese, et al., 1966
WSM	Wiese, et al., 1969

References

Adelman S.J., 1999, A&AS 134, 53
Anderson T., Sorenson G., 1973, JQSRT 13, 369
Basri G., Marcy G.W., 1988, ApJ 330, 274
Berry H.G., Bromander J., Curtis L.J., Buchta R., 1971, Physica Scripta 3, 125
Biemont E., Karner C., Meyer G., Traeger F., zu Putlitz G., 1982, A&AS 107, 166
Bord J.D., Cowley C.R., Norquist P.L., 1997, MNRAS 284, 869
Cowley A.P., Cowley C.R., Jaschek M., Jaschek C., 1969, AJ 74, 375
Dumont P.D., Biemont E., Grevesse N., 1974, JQSRT 14, 1127
Dworetsky M.M., 1980, A&A 84, 350
Dworetsky M.M., Trueman M.R.G., Stickland D.J., 1980, A&A 85, 138
Dworetsky M.M., Storey P.J., Jacobs J.M., 1984, Physica Scripta T8, 39
Fuhr J.R., Martin G.A., Wiese W.L., 1988, J. Phys. Chem. Ref. Data 17, Suppl. 4
Gelbmann M.J., 1998, Cont. Astron. Obs. Skalnaté Pleso 27, 280
Haggkvist L., Oja T., 1969, Ark. Astron. 5, 125
Hauck B., Mermilliod M., 1980, A&AS 40, 1
Hill G.M.R., Blake C.C., 1995, MNRAS 178, 183
Hoffleit D., Jaschek C., 1982, The bright star catalogue. Fourth edition, Yale University
Johnson J.L., Iriarte B., Mitchell R.I., Wisniwsky W.Z., 1966, Comm. Lunar Plan. Lab. 4, 99
Kurucz R.L., 1988, In: McNally M. (ed.) Trans. IAU, XXB, Kluwer, Dordrecht, p. 168
Kurucz R.L., 1993, Synthesis Programs and Line Data (Kurucz CD-ROM No.18)
Kurucz R.L., Peytremann E., 1975, Smithsonian Astrophysical Observatory Special Rep. 362
Landstreet J.D., 1982, ApJ 258, 639
Landstreet J.D., Barker P.K., Bohlender D.A., Jewison M.S., 1989, ApJ 344, 876
Leckrone D.S., Wahlgren G.M., Johansson S., 1991, ApJ 377, L37
Martin G.A., Fuhr J.R., Wiese W.L., 1988, J. Phys. Chem. Ref. Data 17, Suppl. 3
Mathys G., 1990, A&AS 232, 151
Mathys G., Hubrig S., Landstreet J.D., Lanz T., Manfroid J., 1997, A&AS 123, 353
Meggers W.F., Corliss C.H., Schriber B.F., 1975, NBS Monograph 145
Migdalek J., 1976, Can. J. Phys. 54, 2272
Miles B.M., Wiese W.L., Younger S.M., 1981, J. Phys. Chem. Ref. Data 10, 305
Moon T.T., Dworetsky M.M., 1985, PASJ 44, 125
Moore C.E., 1971, NSRDS-NBS 35
Napiwotzki R., Schönberner D., Wenske V., 1993, A&A 268, 653
Palmer D.R., Walker E.N., Jones D.H.P., Wallis R.E., 1968, Roy. Obs. Bull. No. 135
Rosberg M., Wyart J.F., 1997, Physica Scripta 55, 690
Saar S.H., 1988, ApJ 324, 441
Sadakane K., 1992, PASJ 44, 125
Schultz-Gulde E., 1969, JQSRT 9, 13
Sletteback A., Collins II G.W., Boyce P.B., White N.M., Parkinsson T.D., 1975, ApJS 29, 137
Sugar J., Corliss C., 1985, J. Phys. Chem. Ref. Data 14, Suppl. 2
Valenti J.A., Marcy G.W., Basri G., 1995, ApJ 439, 939
Wahlgren G.M., Dolk L., Kalus G., et al., 2000, ApJ, submitted
Wiese W.L., Fuhr J.R., 1975, J. Phys. Chem. Ref. Data 4, 263
Wiese W.L., Smith M.W., Glennon B.M., 1966, NSRDS-NBS 4
Wiese W.L., Smith M.W., Miles B.M., 1969, NSRDS-NBS 22
Wyart J.F., 1997, Physica Scripta 56, 446